

# Biokinetics and Dosimetry of $^{177}\text{Lu}$ -Pentixather

Heribert Hänscheid<sup>1</sup>, Andreas Schirbel<sup>1</sup>, Philipp Hartrampf<sup>1</sup>, Sabrina Kraus<sup>2</sup>, Rudolf A. Werner<sup>1</sup>, Hermann Einsele<sup>2</sup>, Hans-Jürgen Wester<sup>3</sup>, Michael Lassmann<sup>1</sup>, Martin Kortüm<sup>2</sup>, and Andreas K. Buck<sup>1</sup>

<sup>1</sup>Department of Nuclear Medicine, University Hospital Würzburg, Würzburg, Germany; <sup>2</sup>Department of Internal Medicine II, University Hospital Würzburg, Würzburg, Germany; and <sup>3</sup>Department of Pharmaceutical Radiochemistry, TU Munich, Munich, Germany

The chemokine receptor 4 (CXCR4), which is overexpressed in many solid and hematologic malignancies, can be targeted for radioligand therapy via the antagonist pentixather. The biokinetics and dosimetry of  $^{177}\text{Lu}$ -pentixather and  $^{90}\text{Y}$ -pentixather were analyzed in this study.

**Methods:** This retrospective study was a standardized reevaluation of data collected for treatment planning. Nineteen patients with complete sets of planar whole-body scans over at least 4 d and a single SPECT/CT scan after administration of 200 MBq of  $^{177}\text{Lu}$ -pentixather were included. Kinetics were measured in the whole body, in tissues with activity retention, and in 10 individuals in the blood. Time-integrated activity coefficients and tissue-absorbed doses were derived. **Results:** Increased uptake of pentixather was observed in the kidneys, liver, spleen, and bone marrow, inducing respective median absorbed doses of 0.91 Gy (range, 0.38–3.47 Gy), 0.71 Gy (range, 0.39–1.17 Gy), 0.58 Gy (range, 0.34–2.26 Gy), and 0.47 Gy (range, 0.14–2.33 Gy) per GBq of  $^{177}\text{Lu}$ -pentixather and 3.75 Gy (range, 1.48–12.2 Gy), 1.61 Gy (range, 1.14–2.97 Gy), 1.66 Gy (range, 0.97–6.69 Gy), and 1.06 Gy (range, 0.27–4.45 Gy) per GBq of  $^{90}\text{Y}$ -pentixather. In most tissues, activity increased during the first day after the administration of  $^{177}\text{Lu}$ -pentixather and afterward decayed with mean effective half-lives of  $41 \pm 10$  h (range, 24–64 h) in the kidneys and median half-lives of 109, 86, and 92 h in the liver, spleen, and bone marrow, respectively. Maximum uptake per kidney was  $2.2\% \pm 1.0\%$  (range, 0.6%–5.1%). In organs showing no specific uptake, absorbed doses exceeding 0.3 Gy/GBq of  $^{90}\text{Y}$ -pentixather were estimated for the urinary bladder and for tissues adjacent to accumulating organs such as the adrenal glands, bone surface, and gallbladder. Dose estimates for tumors and extramedullary lesions ranged from 1.5 to 18.2 Gy/GBq of  $^{90}\text{Y}$ -pentixather. **Conclusion:** In patients with hematologic neoplasms, absorbed doses calculated for bone marrow and extramedullary lesions are sufficient to be effective as an adjunct to high-dose chemotherapies before stem cell transplantation.

**Key Words:** pentixather; biokinetics; dosimetry; CXCR4; endoradiotherapy

J Nucl Med 2022; 63:754–760

DOI: 10.2967/jnumed.121.262295

The chemokine receptor 4 (CXCR4) influences the development of malignant diseases by activating various signaling pathways that influence cell proliferation, angiogenesis, metastasis, and therapeutic resistance (1). On the other hand, being overexpressed in many solid and hematologic neoplasms, CXCR4 is a promising target structure for radioligand therapy (2). A CXCR4 antagonist that has

already been used in the therapy of various malignant diseases is the peptide pentixather labeled with  $^{177}\text{Lu}$  or  $^{90}\text{Y}$  (3–8). Pentixather and its  $^{177}\text{Lu}$ - and  $^{90}\text{Y}$ -complexes exhibit high selectivity and specificity and good binding affinities to human CXCR4 (4). In blood,  $^{177}\text{Lu}$ -pentixather shows high binding to serum albumin, CXCR4-mediated binding to leukocytes and platelets, and excellent metabolic stability with virtually no tracer degradation (4).

The present report provides the results of a uniformly performed dosimetric reevaluation of measurements after pretherapeutic administration of  $^{177}\text{Lu}$ -pentixather to 19 patients. This compound was originally intended to be used for both dosimetry and therapy. The nuclide  $^{177}\text{Lu}$  has continued to be used for dosimetry and  $^{90}\text{Y}$  for therapy because  $^{90}\text{Y}$ -pentixather proved to be preferable for therapy, pretherapeutic dosimetry with low  $^{90}\text{Y}$  activities is not possible, and pentixather labeled with a diagnostic nuclide such as  $^{111}\text{In}$  has not yet been produced and tested.

## MATERIALS AND METHODS

### Patients

All patients with dosimetric studies with  $^{177}\text{Lu}$ -pentixather and measurements up to at least 4 d after the administration from June 2014 to December 2019 were considered for this retrospective analysis. A boy aged 8 y was excluded, although no obvious differences in activity kinetics were apparent as compared with adults. After excluding 1 study that had to be repeated, 19 studies were eligible for inclusion. The patients (11 women, 8 men; age range, 40–75 y; mean  $\pm$  SD,  $60 \pm 9$  y) had multiple myeloma ( $n = 9$ ), acute myeloid leukemia ( $n = 3$ ), diffuse large B-cell lymphoma ( $n = 2$ ), pre-B acute lymphoblastic leukemia ( $n = 1$ ), T-cell leukemia ( $n = 1$ ), adrenocortical carcinoma ( $n = 2$ ), or thymoma ( $n = 1$ ) and had been treated before by multiple lines of chemotherapy ( $n = 19$ ), stem-cell transplantation (autologous,  $n = 10$ ; allogeneic,  $n = 5$ ), or external-beam radiation therapy ( $n = 9$ ). One patient (patient 7) had only 1 kidney. Details on the included individuals are shown in Table 1.

At the time of study inclusion, all patients had refractory disease and had exhausted the standard treatment options. On the basis of the German Drug Law, §13(2b), and after evaluation by an interdisciplinary panel of specialists, the potential benefit of CXCR4-targeted endoradiotherapy in combination with high-dose chemotherapy and stem-cell transplantation was investigated. All patients gave written informed consent, and the local ethics committee expressed no objections to the retrospective evaluation and publication of the data in accordance with data protection regulations (reference number 20200915 01).

### Radiochemistry

For pretherapeutic dosimetry,  $^{177}\text{Lu}$ -pentixather is synthesized by adding a solution of 75  $\mu\text{g}$  of pentixather (PentixaPharm) and 3.5  $\mu\text{g}$  of gentisic acid in 525  $\mu\text{L}$  of sodium acetate buffer solution (0.4 M, pH 5.2) to a vial containing about 300 MBq of no-carrier-added  $^{177}\text{LuCl}_3$  (ITG; isomeric purity,  $<10^{-7}$   $^{177\text{m}}\text{Lu}$ ) in 200  $\mu\text{L}$  of 0.04 M

Received Mar. 15, 2021; revision accepted Aug. 5, 2021.

For correspondence or reprints, contact Heribert Hänscheid (haenscheid\_h@ukw.de).

Published online Aug. 19, 2021.

COPYRIGHT © 2022 by the Society of Nuclear Medicine and Molecular Imaging.

**TABLE 1**  
Patient Characteristics at Time of Dosimetric Assessment with <sup>177</sup>Lu-Pentixather

Patient no.	Sex	Age (y)	Weight (kg)	Height (cm)	eGFR	Disease	Since (mo)	Previous treatment			
								C	R	Auto	Allo
1	M	61	60	158	99	MM	18	x		1	
2	F	66	64	163	100	MM	54	x		3	
3	F	53	74	165	54	MM	123	x		3	
4	M	65	93	192	46	MM	101	x		2	
5	M	74	60	173	54	MM	22	x	x	2	
6	M	71	80	175	79	MM	77	x	x	2	
7	F	66	60	166	40	MM	138	x	x	1	
8	F	57	104	157	96	MM	49	x	x	1	
9	M	59	77	172	50	MM	23	x	x	2	
10	M	46	70	183	92	AML	7	x			1
11	M	60	78	182	82	AML	19	x			1
12	F	54	62	168	67	AML	27	x			1
13	F	64	80	163	85	DLBCL	42	x			1
14	F	59	68	172	20	DLBCL	32	x	x	1	
15	F	75	75	168	59	pre-B ALL	15	x			
16	F	50	78	172	54	TCL	21	x			1
17	F	55	64	160	96	ACC	46	x	x		
18	M	55	90	175	92	ACC	14	x	x		
19	F	40	52	163	n/a	Thymoma	37	x	x		

eGFR = Chronic Kidney Disease Epidemiology Collaboration glomerular filtrate rate estimate in mL/min per 1.73 m<sup>2</sup>; C = chemo; R = irradiation; auto = autologous stem cells; allo = allogeneic stem cells; MM = multiple myeloma; AML = acute myeloid leukemia; DLBCL = diffuse large B-cell lymphoma; pre-B ALL = pre-B acute lymphoblastic leukemia; TCL = T-cell leukemia; ACC = adrenocortical carcinoma; n/a = not available.

HCl and heating the vial for 35 min at 100°C. After cooling, the solution is diluted with saline, passed through a 0.22-mm sterile filter, and tested for radiochemical purity by gradient high-performance liquid chromatography and thin-layer chromatography. Bubble point and pH value are determined before releasing the product.

The radiosynthesis of <sup>90</sup>Y-pentixather for therapy follows the same protocol but using higher amounts of pentixather (200 µg), gentisic acid (7 µg), and radioactivity (2–10 GBq of <sup>90</sup>YCl<sub>3</sub>).

#### Measurements and Data Evaluation

Each patient received about 200 MBq of <sup>177</sup>Lu-pentixather (Supplemental Table 1; supplemental materials are available at <http://jnm.snmjournals.org>) for pretherapeutic dosimetry to confirm eligibility for treatment and to determine the maximum therapeutic activity. The radiopharmaceutical was administered without concomitant medication to protect the kidneys. Activity kinetics were analyzed in the whole body, kidney, liver, spleen, red marrow, and tumorous lesions from repeated whole-body scans and a SPECT/CT scan for normalization to absolute activity concentrations.

Whole-body scanning was performed with the same dual-head γ-camera and identical camera settings at 0.1 h, 4 h, 1 d, 2 d, and 4 d or later after the activity administration. Additional scans after 1 h or 3 d were included if available. For accumulating tissues, net counts were extracted from appropriate regions of interest and fitted by a decay function using ordinary least-squares regression (“Whole-Body Scans” section in supplemental materials; Supplemental Figs. 1 and 2).

Total-body net counts were normalized to the net counts observed in the first scan at 0.1 h. For other tissues, estimates of time-integrated activity coefficients and the specific absorbed doses, that is, the absolute absorbed doses per unit administered activity, were deduced by normalizing the kinetics to activity concentrations measured 1 d (2 d in patient 9) after the administration by SPECT/CT (“Tomographic Imaging” section in supplemental materials; Supplemental Fig. 3).

When possible, activity in entire organs was quantified in SPECT/CT. In large organs, livers, and enlarged spleens, activity was quantified in a partial volume and activity was scaled to the complete mass measured by CT. For the red bone marrow, the activity–time function was determined in the planar images with a large region of interest over the pelvis and spine and normalized to the activity measured on SPECT/CT in the L2–L4 spine, which was assumed to contain 6.7% of the total red marrow activity (9).

In a subgroup of 10 patients, blood samples were collected concomitantly with the whole-body scans. The whole-blood activity concentrations were measured, and the time-integrated activity coefficients per liter of blood were calculated by integration of a triexponential fit function over time.

From the kinetics measured with <sup>177</sup>Lu-pentixather, those expected for <sup>90</sup>Y-pentixather were calculated by converting the decay constants to the shorter physical half-life of <sup>90</sup>Y (64.0 h instead of 159.5 h for <sup>177</sup>Lu).

The free internal dosimetry software IDAC-DOSE (version 2.1 (10)) was used to determine specific absorbed doses in evaluated

tissues from the measured time-integrated activity coefficients per unit mass scaled to the sex-specific reference masses and multiplied by the organ- and sex-specific S values in IDAC-DOSE. The software was also used to estimate absorbed doses in unevaluated tissues from the medians of the measured time-integrated activity coefficients and the kidney–bladder model as previously described (11) with a 3.5-h voiding interval. The percentage of total-body activity not located in the evaluated accumulating tissues was attributed to the remainder of the body.

The free software JASP (version 0.14.1; <https://jasp-stats.org/>) was used for statistical analyses. The distributions determined in this study were tested for normality using the Shapiro–Wilk test, with rejection of the null hypothesis for *P* values of less than 0.05. Parameters of normally distributed data are reported as mean  $\pm$  SD and range or as median and quartiles (minimum, first quartile, third quartile, and maximum).

## RESULTS

The biokinetics of  $^{177}\text{Lu}$ -pentixather were heterogeneous in the group of included patients. Figure 1 shows the whole-body scans 2 d after the administration of the diagnostic activity in 3 of the patients: patient 7, with only 1 kidney, showed the highest specific absorbed doses in the kidney and liver; patient 15, with pre-B acute lymphoblastic leukemia, showed the highest specific absorbed dose in the red marrow and spleen, as well as the highest whole-body time-integrated activity coefficient; and patient 2, with multiple myeloma, showed the highest specific absorbed dose in an extramedullary lesion and the highest time-integrated activity coefficient per liter of blood.

Tables 2 and 3 list the time-integrated activity coefficients and specific absorbed doses for the evaluated tissues for  $^{177}\text{Lu}$ -pentixather and  $^{90}\text{Y}$ -pentixather, respectively. Figure 2 shows typical

time functions of activity retention in organs and tissues, exemplified by patient 3.

The red bone marrow was the dose-limiting organ when the absorbed dose was limited to 2 Gy to preserve function. The mean effective half-life in the bone marrow was  $97 \pm 31$  h (range, 39 h to physical half-life) after  $^{177}\text{Lu}$  (kinetics decay-corrected to  $^{90}\text{Y}$ :  $50 \pm 9$  h; range, 29 to physical half-life). In 14 patients, the red marrow activity concentration initially increased and reached a maximum at  $23 \pm 11$  h after the administration before decreasing.

If stem cell support is available and myeloablation is tolerated or intended, the therapeutic activity is limited not by the red marrow but by the absorbed dose to the kidneys (23 Gy). This would have increased the tolerable activity by a median factor of 4.9 (range, 1.6–70.9) after  $^{177}\text{Lu}$  and a factor of 2.8 (range, 1–34.7) after  $^{90}\text{Y}$  even without kidney-protective medication. Uptake per kidney generally increased at 4 h and later up to a mean maximum of  $2.2\% \pm 1.0\%$  (range, 0.6%–5.1%) of the administered activity at  $18 \pm 7$  h after the administration and a subsequent decrease with a mean effective half-life of  $41 \pm 10$  h (range, 24–64 h). The fitted half-life of the increasing component was 27 h in patient 7 and a median of 7.8 h (quartiles: 2.4, 4.9, 12.2, and 15.4 h) in patients with 2 kidneys. Decay-corrected to  $^{90}\text{Y}$ , the mean maximum uptake would have been  $1.9\% \pm 0.9\%$  (range, 0.5%–4.0%) after  $14 \pm 6$  h, and the mean effective half-life would have been  $29 \pm 5$  h (range, 20–40 h).

Compared with the kidney, the kinetics in the liver were retarded, with a later maximum of retention ( $6.1\% \pm 1.8\%$ ; range, 2.2%–10.0%) after  $35 \pm 11$  h and a longer median effective half-life of 109 h (quartiles: 77 h, 92 h, 146 h, and physical half-life) after  $^{177}\text{Lu}$ . Respective data for  $^{90}\text{Y}$ -pentixather would have been  $4.9\% \pm 1.6\%$  (range, 1.8%–8.6%) retention after  $23 \pm 7$  h and a

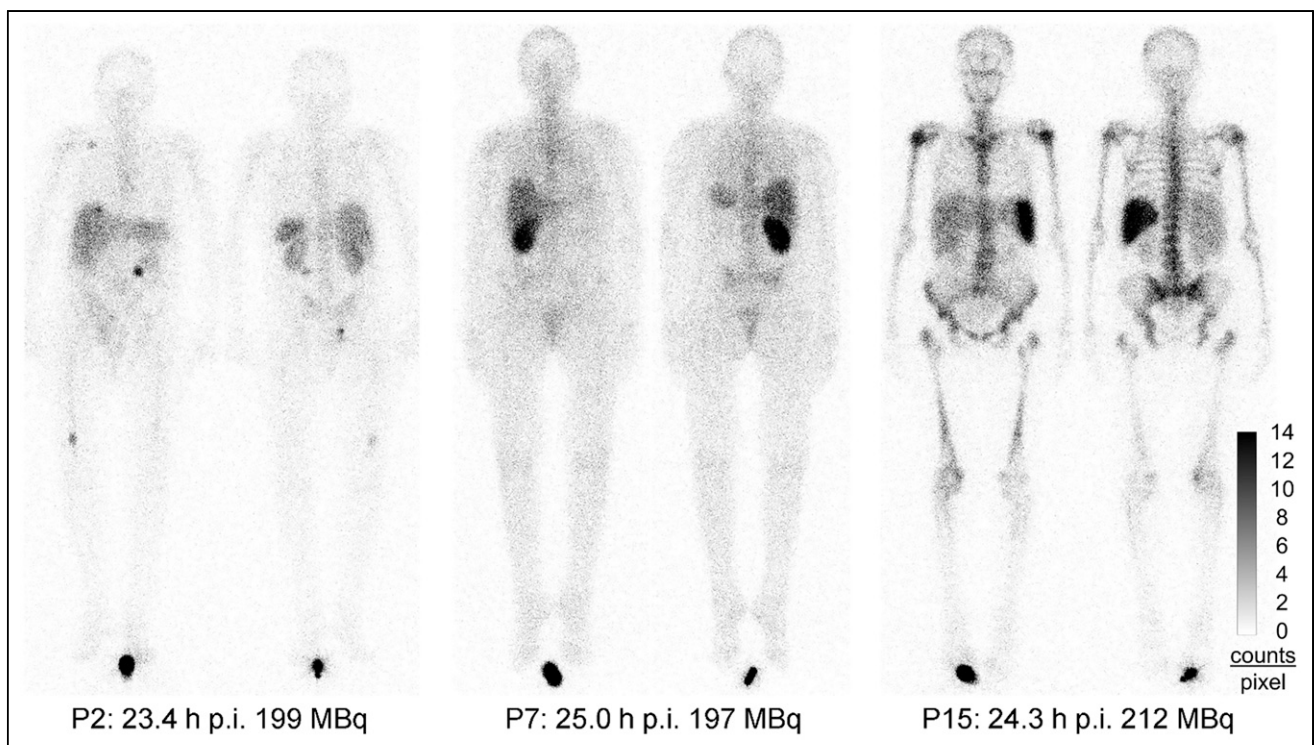


**FIGURE 1.** Examples of different activity distributions after  $^{177}\text{Lu}$ -pentixather in patients 2 and 7 (P2 and P7, respectively), with multiple myeloma, and patient 15 (P15), with pre-B acute lymphoblastic leukemia. Although uptake in single kidney of patient 7 was 5%, sum of uptakes in both kidneys of patient 15 was only 1.1%. In contrast, retention was 3-fold higher in bone marrow and 11-fold higher in spleen of patient 15. p.i. = after injection.

**TABLE 2**

<sup>177</sup>Lu-Pentixather Time-Integrated Activity Coefficients in Whole Body, Organs, Tumorous Lesions, Red Marrow, and Blood, as Well as Tissue-Absorbed Doses per Administered Activity in Organs and Lesions

Patient no.	WB	Kidneys		Liver		Spleen		Red marrow		Lesion	Blood
	$\bar{a}$ (h)	$\bar{a}$ (h)	D/A (Gy/GBq)	$\bar{a}$ (h)	D/A (Gy/GBq)	$\bar{a}$ (h)	D/A (Gy/GBq)	$\bar{a}$ (h)	D/A (Gy/GBq)	D/A (Gy/GBq)	$\bar{a}$ (h/L)
1	51.6	4.39	1.01	3.8	0.39	2.06	0.58	4.0	0.14	2.2	0.21
2	56.1	2.42	0.71	14.4	0.82	2.49	1.55	8.1	0.37	6.9	0.58
3	55.3	4.85	2.10	15.2	0.93	1.27	0.72	14.3	0.66		0.48
4	97.6	4.61	1.48	16.2	0.80	2.03	0.70	13.7	0.48		0.28
5	87.7	1.92	0.87	12.2	0.91	3.71	1.59	16.8	0.59	1.7	
6	62.1	1.74	0.50	11.7	0.62	0.63	0.34	11.8	0.41	3.1	
7	111.0	6.25	3.47	15.0	1.17	1.34	1.12	10.6	0.48		
8	61.6	5.28	1.21	10.0	0.39	0.90	0.38	9.4	0.43		
9	111.6	4.76	1.12	13.2	0.67	1.18	0.47	13.6	0.47		
10	50.5	4.51	0.90	9.0	0.43	2.47	0.40	9.9	0.35		0.32
11	55.9	4.34	1.14	8.0	0.42	1.43	0.48	9.1	0.32		0.34
12	77.8	2.03	0.79	13.9	0.71	3.46	0.75	21.3	0.97	1.1	
13	114.9	7.87	0.91	21.9	0.67	2.65	0.35	22.8	1.04	2.1	
14	83.6	1.63	0.59	16.7	0.88	11.5	1.20	16.4	0.75		
15	140.9	1.04	0.38	15.5	0.71	14.0	2.26	51.0	2.33		
16	108.8	3.22	1.07	14.1	0.50	6.51	1.03	12.2	0.56	1.6	0.28
17	73.6	1.93	0.52	20.1	0.92	2.38	0.56	5.5	0.25	2.3	0.28
18	51.6	3.47	0.67	12.0	0.41	3.30	0.42	4.0	0.14	1.1	0.32
19	48.0	5.23	1.96	9.4	0.81	0.44	0.48	8.5	0.39	0.7	0.44
<i>P</i>	0.03	0.31	<0.01	0.95	0.21	<0.01	< 0.01	<0.01	<0.01	< 0.01	0.23
Minimum	48.0	1.04	0.38	3.7	0.39	0.44	0.34	4.0	0.14	0.7	0.21
First quartile	55.6	1.98	0.70	10.9	0.47	1.30	0.45	8.8	0.36	1.2	0.28
Median	73.6	4.34	0.91	13.9	0.71	2.38	0.58	11.8	0.47	1.9	0.32
Third quartile	103.2	4.80	1.18	15.4	0.85	3.38	1.08	15.4	0.62	2.3	0.42
Maximum	140.9	7.87	3.47	21.9	1.17	14.0	2.26	51.0	2.33	6.9	0.58
Mean	79.0	3.77	1.13	13.3	0.69	3.36	0.81	13.8	0.59	2.3	0.35
SD	27.9	1.82	0.73	4.2	0.22	3.61	0.52	10.4	0.49	1.8	0.11

WB = whole body;  $\bar{a}$  = time-integrated activity coefficient; D/A = tissue-absorbed doses per administered activity. *P* values are from Shapiro–Wilk test of normality.

median effective half-life of 54 h (quartiles: 45 h, 49 h, 54 h, and physical half-life).

High values for the time-integrated activity coefficient for the spleen (Tables 2 and 3) were associated with splenomegaly due to malignant infiltration. In affected patients, a high absorbed dose to the spleen is considered a desirable therapeutic effect. Measured spleen masses in patients 14, 15 (Fig. 1), and 16 were 824, 530, and 539 g, respectively. Fifteen patients showed a delayed retention maximum. The mean effective half-life in the spleen was  $99 \pm 36$  h (range, 51 h to physical half-life) after <sup>177</sup>Lu (<sup>90</sup>Y:  $50 \pm 9$  h; range, 35 h to physical half-life).

In malignant extramedullary lesions, activity initially almost always increased, reaching a maximum after a median of 11 h and then decreasing with effective half-lives of  $122 \pm 32$  h (range, 78 h to physical half-life) after <sup>177</sup>Lu (<sup>90</sup>Y:  $56 \pm 7$  h; range, 45 h to

physical half-life). The calculated values for the tissue-absorbed doses per unit administered activity ranged from 0.7 to 6.9 Gy/GBq of <sup>177</sup>Lu and from 1.5 to 18.2 Gy/GBq of <sup>90</sup>Y.

Estimates of absorbed doses in organs apparently without specific activity accumulation are shown in Supplemental Table 2. Absorbed doses of about 0.05 Gy/GBq of <sup>177</sup>Lu-pentixather and 0.2 Gy/GBq of <sup>90</sup>Y-pentixather are expected in most organs. Somewhat higher values are estimated for the urinary bladder and for tissues adjacent to accumulating organs such as the adrenals, bone surface, and gallbladder.

**DISCUSSION**

High and long-lasting retention of pentixather in the bone marrow leads to high specific absorbed doses to the hematopoietic

TABLE 3

<sup>90</sup>Y-Pentixather Time-Integrated Activity Coefficients in Whole Body, Organs, Tumorous Lesions, Red Marrow, and Blood, as Well as Tissue-Absorbed Doses per Administered Activity in Organs and Lesions (Recalculated from Kinetics Measured with <sup>177</sup>Lu-Pentixather)

Patient no.	WB	Kidneys		Liver		Spleen		Red marrow		Lesion	Blood
	$\bar{a}$ (h)	$\bar{a}$ (h)	D/A (Gy/GBq)	$\bar{a}$ (h)	D/A (Gy/GBq)	$\bar{a}$ (h)	D/A (Gy/GBq)	$\bar{a}$ (h)	D/A (Gy/GBq)	D/A (Gy/GBq)	$\bar{a}$ (h/L)
1	31.5	3.03	3.91	1.9	1.18	1.05	1.66	2.3	0.34	6.1	0.19
2	33.6	1.90	3.16	5.8	1.91	0.95	3.30	4.0	0.77	18.2	0.48
3	35.1	2.95	7.32	6.0	2.12	0.53	1.70	7.4	1.42		0.42
4	51.6	2.97	5.36	6.3	1.80	0.82	1.58	6.0	0.88		0.28
5	50.8	1.22	3.10	6.1	2.65	1.26	3.04	8.4	1.23	4.1	
6	40.1	1.31	2.12	5.2	1.61	0.40	1.20	7.4	1.09	9.2	
7	54.2	3.87	12.2	6.6	2.97	0.69	3.22	6.5	1.25		
8	34.5	3.74	4.85	5.4	1.22	0.45	1.07	5.1	0.98		
9	58.5	3.22	4.29	6.1	1.77	0.67	1.51	7.2	1.06		
10	32.8	3.32	3.75	4.6	1.29	1.07	0.97	4.9	0.72		0.28
11	35.7	2.83	4.21	3.8	1.16	0.76	1.42	4.7	0.69		0.30
12	47.2	1.41	3.16	5.4	1.61	2.06	2.51	10.1	1.94	3.4	
13	59.3	4.89	3.21	8.5	1.51	1.42	1.05	8.9	1.72	4.7	
14	49.6	1.04	2.15	7.6	2.32	6.63	3.85	9.6	1.85		
15	67.7	0.71	1.48	6.0	1.57	7.40	6.69	23.2	4.45		
16	63.8	2.38	4.50	7.8	1.59	3.04	2.70	7.1	1.36	4.2	0.26
17	41.1	1.39	2.15	8.7	2.31	1.41	1.88	3.1	0.59	5.4	0.44
18	34.5	2.47	2.67	5.7	1.14	1.58	1.13	1.8	0.27	3.6	0.28
19	29.9	3.53	7.52	3.6	1.80	0.25	1.53	3.5	0.68	1.5	0.40
<i>P</i>	0.08	0.53	<0.01	0.55	0.13	<0.01	<0.01	<0.01	<0.01	<0.01	0.31
Minimum	29.9	0.71	1.48	2.0	1.14	0.25	0.97	1.83	0.27	1.5	0.19
First quartile	34.5	1.40	2.88	5.3	1.40	0.68	1.31	4.35	0.71	3.7	0.28
Median	41.1	2.83	3.75	6.0	1.61	1.05	1.66	6.50	1.06	4.5	0.29
Third quartile	52.9	3.27	4.67	6.4	2.02	1.50	2.87	7.88	1.39	5.9	0.41
Maximum	67.7	4.89	12.2	8.7	2.97	7.40	6.69	23.2	4.45	18.2	0.48
Mean	44.8	2.54	4.27	5.9	1.77	1.71	2.21	6.90	1.22	6.0	0.33
SD	12.0	1.14	2.52	1.7	0.51	1.99	1.39	4.61	0.91	4.7	0.10

WB = whole body;  $\bar{a}$  = time-integrated activity coefficient; D/A = tissue-absorbed doses per administered activity. *P* values are from Shapiro–Wilk test of normality.

system. The estimates for the bone marrow–absorbed dose indicate that the safety limit of 2 Gy is usually reached after about 4 GBq of <sup>177</sup>Lu or 2 GBq of <sup>90</sup>Y. The absorbed doses achievable in malignant tissues with these activities are considered insufficient to achieve an adequate therapeutic effect on malignant tissue, especially in solid tumors with moderate CXCR4 expression. In hematologic neoplasms, on the other hand, therapy with pentixather can be a reasonable complement to high-dose chemotherapy regimens followed by subsequent hematopoietic stem cell transplantation, with the potential to effectively fight radiation-sensitive lesions.

With the exception of patients 11, 14, and 15, who experienced unexpected obstacles regarding stem cell availability, and patient

5, whose health deteriorated, all patients with hematologic diseases received therapy. Patients 17, 18, and 19, with adrenocortical carcinoma or thymoma, remained untreated. Patients 1–4 received <sup>177</sup>Lu-pentixather for treatment (“Posttherapeutic Measurements” section in the supplemental materials; Supplemental Figs. 4 and 5), and all others received <sup>90</sup>Y-pentixather. <sup>177</sup>Lu-pentixather for therapy has the advantage that its  $\gamma$ -radiation can be used scintigraphically for verification of the activity distribution and for dosimetry, but <sup>177</sup>Lu-pentixather has an unfavorably long half-life in the bone marrow. With therapeutic doses of 10 Gy or more to the red bone marrow, the activity in the marrow must decay for at least 4–5 half-lives before stem cell transplantation to safely avoid compromising engraftment. Although this level of decay is ensured 2 wk after



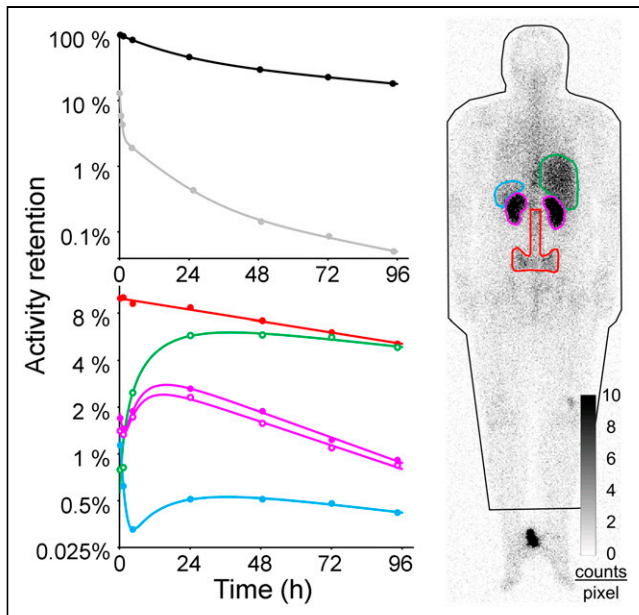


**FIGURE 2.** Regions of interest used to derive time functions of activity retention in whole body (black), red bone marrow (red), liver (green), right kidney (purple solid circles), left kidney (purple open circles), and spleen (blue) in patient 3 with respective fit functions. Scintigram shows posterior whole-body image 24 h after 197 MBq of  $^{177}\text{Lu}$ -pentixather. Gray symbols with fit function represent activity retention per liter of whole blood.

$^{90}\text{Y}$ -pentixather, an interval of up to 4 wk may be necessary for  $^{177}\text{Lu}$ -pentixather. The longer time between  $^{177}\text{Lu}$ -pentixather treatment and transplantation is disadvantageous because the prolonged phase of aplasia poses an increased risk of infectious complications.

Since pentixather, like other radiolabeled peptides, is filtered through the kidneys, activity retention in the renal tubules must be considered. It is not yet known whether  $^{90}\text{Y}$ , like somatostatin receptor agonists, has higher renal toxicity because of its higher  $\beta$ -energy and dose rate, nor is it known which renal dose limits are appropriate for pentixather labeled with  $^{177}\text{Lu}$  or  $^{90}\text{Y}$ . The limit of 23 Gy for the tolerable absorbed dose, which is often used for the kidneys (12), is reached after 20–30 GBq of  $^{177}\text{Lu}$ -pentixather or 5–8 GBq of  $^{90}\text{Y}$ -pentixather in most patients. Although 10 GBq of  $^{90}\text{Y}$ -pentixather could have been safely administered in 20% of patients, the specific absorbed dose determined for the patient with only 1 kidney (patient 7) was 12.2 Gy/GBq, limiting the safely administrable activity to 1.9 GBq. In patients with 2 kidneys, who were not included in this study because dosimetric measurements were performed over 3 d only, the highest calculated dose was 12.7 Gy/GBq of  $^{90}\text{Y}$ -pentixather.

Concomitant medication with amino acids, such as that recommended for somatostatin receptor therapy with radiolabeled peptides (12), also reduces retention of pentixather in the kidneys (Supplemental Table 3). The reduction factor of  $64\% \pm 13\%$  (range, 50%–80%) reported previously (8) was derived from only 6 treatments with  $^{177}\text{Lu}$ -pentixather and remains to be validated.

The above figures indicate that, in an approach that uses myeloablative therapy with fixed activities, hardly more than 2.5 GBq of  $^{90}\text{Y}$ -pentixather can be administered without exceeding a kidney dose of 23 Gy in individual patients. The estimated specific

absorbed doses to bone marrow and lesions indicate that this limitation is likely to leave many patients inadequately dosed, which strongly supports the theranostic approach with pretherapeutic dosimetry.

The data in the present study were not collected prospectively in an optimized study design. The dosimetric measurements were performed with the lowest activity that seemed necessary, limiting the accuracy of the scintigraphic imaging and its evaluation (“Uncertainties” section in supplemental materials). Some estimate of the dosimetric accuracy is provided by the intraindividual comparison of the absorbed doses determined for the right and left kidneys after  $^{177}\text{Lu}$ -pentixather, which incorporates the uncertainties of both volume segmentation and measurement and fit of activity kinetics. The dose derived for the right kidney was  $108\% \pm 14\%$  (range, 78%–128%) that derived for the left kidney.

In tissues with a delayed retention maximum and a long half-life for the retained activity, namely the liver, spleen, and red bone marrow, measurements over 4 d are often not sufficient to determine the half-life with good accuracy. Later measurements, however, were not necessary to estimate the absorbed doses to the kidneys and would have required an additional patient visit and the use of higher activities, which were avoided to minimize the risk that the kinetics would be affected by the dose administered pretherapeutically. For therapy with  $^{90}\text{Y}$ -pentixather, scans over 3 d are sufficient to measure the kinetics in the kidneys (“Uncertainties” section in supplemental materials).

$^{90}\text{Y}$ -pentixather kinetics data shown here were not measured but calculated by converting the  $^{177}\text{Lu}$ -pentixather results, assuming comparable kinetics for  $^{nat}\text{Lu}$  and  $^{nat}\text{Y}$ . Comparison of kinetics during therapy with prediction has not been technically possible in our patients treated with  $^{90}\text{Y}$ -pentixather but is intended in the future by quantification of the positrons of the  $^{90}\text{Y}$  decay with a PET/CT scan of higher sensitivity. Since the metal that is used affects the CXCR4 affinity and thus potentially the biokinetics, deviations of actual absorbed doses from estimates are possible. The binding affinity of  $^{nat}\text{Y}$ -pentixather to CXCR4 is slightly lower than that of  $^{nat}\text{Lu}$ -pentixather (4), which is most likely to affect binding in target tissues. Also, an influence on excretion and kinetics in healthy organs cannot generally be excluded.

An interesting alternative for the treatment of hematologic malignancies could be the labeling of pentixather with an  $\alpha$ -emitter to effectively target smaller cell clusters.  $^{nat}\text{Bi}$ -pentixather has a higher binding affinity to CXCR4 than does  $^{nat}\text{Lu}$ -pentixather (4), but even for the most suitable isotope,  $^{213}\text{Bi}$ , the half-life of only 46 min is likely to be too short.

Bone marrow dosimetry is uncertain even in healthy individuals. In patients with malignant transformation of the hematologic system, the bone marrow may be severely modified in an individualized manner. The activity pattern in the medullary spaces is often very inhomogeneous, and the assumption of 6.7% bone marrow content in the evaluated vertebrae is even more uncertain than in healthy subjects. The doses mentioned should therefore be regarded as calculated values for estimating the approximate magnitude.

## CONCLUSION

The absorbed radiation doses achievable with labeled pentixather are often insufficient for radiologic destruction of solid tumors. In hematologic neoplasms, however,  $^{90}\text{Y}$ -pentixather can be effective against radiosensitive lesions and as a useful adjunct to the

conditioning regimen before stem cell transplantation. Although the kidneys are the dose-limiting organ in myeloablative therapy, high exposures also occur in the liver and spleen. Of the remaining organs, absorbed doses exceeding 0.3 Gy/GBq are estimated for the urinary bladder and for tissues adjacent to accumulating organs such as the adrenal glands, bone surface, and gallbladder.

## DISCLOSURE

This publication was funded in part by the CDW-Stiftung, Kassel, Germany. No other potential conflict of interest relevant to this article was reported.

## KEY POINTS

**QUESTION:** How do the biokinetics of the CXCR4 antagonist pentixather affect endoradiotherapy?

**PERTINENT FINDINGS:** Dosimetric studies with 200 MBq of <sup>177</sup>Lu-pentixather in 19 patients demonstrated very heterogeneous absorbed doses per administered activity in organs and tissues and identified the red bone marrow and kidneys as dose-limiting organs.

**IMPLICATIONS FOR PATIENT CARE:** Therapy with <sup>90</sup>Y-pentixather may be considered if the malignant tissue is radiosensitive, myeloablation is accepted, and excessive renal absorbed dose is avoided by pretherapeutic dosimetry.

## REFERENCES

1. Chatterjee S, Behnam Azad B, Nimmagadda S. The intricate role of CXCR4 in cancer. *Adv Cancer Res.* 2014;124:31–82.
2. Walenkamp AME, Lapa C, Herrmann K, Wester HJ. CXCR4 ligands: the next big hit? *J Nucl Med.* 2017;58(suppl):77S–82S.
3. Herrmann K, Schottelius M, Lapa C, et al. First-in-human experience of CXCR4-directed endoradiotherapy with Lu-177- and Y-90-labeled pentixather in advanced-stage multiple myeloma with extensive intra- and extramedullary disease. *J Nucl Med.* 2016;57:248–251.
4. Schottelius M, Osl T, Poschenrieder A, et al. [Lu-177]pentixather: comprehensive preclinical characterization of a first CXCR4-directed endoradiotherapeutic agent. *Theranostics.* 2017;7:2350–2362.
5. Habringer S, Lapa C, Herhaus P, et al. Dual targeting of acute leukemia and supporting niche by CXCR4-directed theranostics. *Theranostics.* 2018;8:369–383.
6. Lapa C, Hanscheid H, Kircher M, et al. Feasibility of CXCR4-directed radioligand therapy in advanced diffuse large B-cell lymphoma. *J Nucl Med.* 2019;60:60–64.
7. Maurer S, Herhaus P, Lippenmeyer R, et al. Side effects of CXCR4-chemokine receptor 4-directed endoradiotherapy with pentixather before hematopoietic stem cell transplantation. *J Nucl Med.* 2019;60:1399–1405.
8. Lapa C, Herrmann K, Schirbel A, et al. CXCR4-directed endoradiotherapy induces high response rates in extramedullary relapsed multiple myeloma. *Theranostics.* 2017;7:1589–1597.
9. Shen S, Meredith RF, Duan J, et al. Improved prediction of myelotoxicity using a patient-specific imaging dose estimate for non-marrow-targeting Y-90-antibody therapy. *J Nucl Med.* 2002;43:1245–1253.
10. Andersson M, Johansson L, Eckerman K, Mattsson S. IDAC-Dose 2.1, an internal dosimetry program for diagnostic nuclear medicine based on the ICRP adult reference voxel phantoms. *EJNMMI Res.* 2017;7:88.
11. ICRP publication 106: radiation dose to patients from radiopharmaceuticals—a third amendment to ICRP publication 53. *Ann ICRP.* 2008;38:1–197.
12. Bodei L, Mueller-Brand J, Baum RP, et al. The joint IAEA, EANM, and SNMMI practical guidance on peptide receptor radionuclide therapy (PRRNT) in neuroendocrine tumours. *Eur J Nucl Med Mol Imaging.* 2013;40:800–816.